

ФІЗИЧНІ, ХІМІЧНІ ТА ІНШІ ЯВИЩА, НА ОСНОВІ ЯКИХ МОЖУТЬ
БУТИ СТВОРЕНІ СЕНСОРИ

PHYSICAL, CHEMICAL AND OTHER PHENOMENA,
AS THE BASES OF SENSORS

PACS CODES: 73.61.EY, 61.10NZ, 61.72.DD, 81.40VW

**EFFECT OF ANNEALING ON DEFECT STRUCTURE
OF GaMnAs AND Si:Mn**

*J. Bak-Misiuk^a, E. Dynowska^a, P. Romanowski^a, A. Misiuk^b,
A. Shalimov^a, J. Z. Domagala^a, E. Lusakowska^a, J. Sadowski^a,
W. Caliebe^c, W. Szuszkiewicz^a, J. Trela^a*

^aInstitute of Physics, PAS, Al. Lotnikow 32/46, 02-668 Warsaw, Poland;
Phone: +48 22 8436034; Fax: +48 22 846034; E-mail: bakmi@ifpan.edu.pl

^bInstitute of Electron Technology, Al. Lotnikow 46, 02-668 Warsaw, Poland;
Phone: +48 22 5487792; Fax: +48 22 8470631; E-mail: misiuk@ite.waw.pl

^cHASYLAB-DESY, Notkerstrasse 85, D-22603, Hamburg, Germany;
Phone: +49 (0)40 8998 1646; E-mail: wolfgang.caliebe@desy.de

Abstract

EFFECT OF ANNEALING ON DEFECT STRUCTURE OF GaMnAs AND Si:Mn

*J. Bak-Misiuk, E. Dynowska, P. Romanowski, A. Misiuk, A. Shalimov, J. Z. Domagala,
E. Lusakowska, J. Sadowski, W. Caliebe, W. Szuszkiewicz, J. Trela*

Effect of annealing on defect structure of thin GaMnAs layers and on Si implanted with Mn⁺ (Si:Mn) has been investigated by X-ray methods, Atomic Force Microscopy and Secondary Ion Mass Spectroscopy. Before and after the treatment the layers were fully strained in respect to the substrate. Decreased value of the GaMnAs lattice parameter is probably related to a decrease in concentration of As antisites and of Mn interstitials and created of MnAs clusters. Lattice parameter of annealed GaMnAs with 2% Mn content was smaller than that of GaAs substrate. Mn concentration remains unchanged after annealing. Defect structure of Si:Mn depends on treatment parameters.

Keywords: GaMnAs, Si, X-ray diffraction, thin layers, implantation, pressure, annealing, spintronics.

Анотація

ВПЛИВ ВІДПАЛУ НА СТРУКТУРУ ДЕФЕКТІВ GaMnAs І Si:Mn

*Й. Бак-Мисюк, Е. Діновська, П. Романовські, А. Мисюк, А. Шалімов, Й. З. Домагала,
Е. Лукаковська, Й. Садовські, В. Калебе, В. Шушкевич, Й. Трела*

Вплив відпалу на структуру дефектів тонких шарів GaMnAs і на кремній, легований Mn⁺ (Si:Mn) було досліджено методами рентгеноскопії, атомної мікроскопії та мас-спектроскопії вторинних іонів. До і після обробки рівні були повністю деформовані відносно підкладки. Зменшення значення параметра кристалічної ґратки GaMnAs ймовірно пов'язане зі зменшенням концентрації заміщень As і міжвузлового Mn і створенням кластерів MnAs. Параметр кристалічної ґратки відпаленого GaMnAs з 2%-ним змістом Mn був менше, ніж параметр кристалічної ґратки підкладки GaAs. Концентрація Mn після відпалу залишилася незмінною. Дефектна структура Si:Mn залежить від параметрів відпалу.

Ключові слова: GaMnAs, Si, рентгенівська дифракція, тонкі шари, імплантація, тиск, відпал, спінтроніка.

Аннотация

ВЛИЯНИЕ ОТЖИГА НА СТРУКТУРУ ДЕФЕКТОВ GaMnAs И Si:Mn

*Й. Бак-Мисюк, Е. Диновска, П. Романовски, А. Мисюк, А. Шалимов, Й. З. Домагала,
Е. Лукаковска, Й. Садовски, В. Калебе, В. Шушкевич, Й. Трела*

Влияние отжига на структуру дефектов тонких слоев GaMnAs и на кремний, легированный Mn⁺ (Si:Mn) было исследовано методами рентгеноскопии, атомной микроскопии и масс-спектроскопии вторичных ионов. До и после обработки уровни были полностью деформированы относительно подложки. Уменьшение значения параметра кристаллической решетки GaMnAs вероятно связано с уменьшением концентрации замещений As и междоузельного Mn и созданием кластеров MnAs. Параметр кристаллической решетки отожженного GaMnAs с 2%-ым содержанием Mn был меньше, чем параметр кристаллической решетки подложки GaAs. Концентрация Mn после отжига осталась неизменной. Дефектная структура Si:Mn зависит от параметров отжига.

Ключевые слова: GaMnAs, Si, рентгеновская дифракция, тонкие слои, имплантация, давление, отжиг, спинтроника.

Introduction

In recent years a rapid development of spintronics is observed. This exciting new field of research combines magnetism and electronics (or optoelectronics). The goal is to create conceptually new devices utilizing spin of electron.

The key to the spintronics success is availability of suitable materials for device manufacturing. Following features of such materials are desired: their band structure should be strongly dependent on electron spin polarization, injection of spin-polarized electrons should be possible, and certainly they should be easily integrated into circuits (ICs). Unfortunately, the presently available magneto-electronic devices are based on metallic multi-layers, integration of which into common ICs is not easy and injection of

spin-polarized electron into attached semiconductor is not very effective. On the other hand, typical semiconductors are nonmagnetic. The natural choice are so called diluted magnetic semiconductors (DMS), i.e. mixed crystals based on classical semiconductors, with a controlled fraction of nonmagnetic cations being substituted by magnetic ions [1, 2]. It is believed that the best candidates for spintronic materials are DMS based on III-V semiconducting compounds, since they can be doped for both p- and n-types, relatively easily integrated into ICs; ferromagnetism has been found for some of them [2, 3]. Obviously the room temperature ferromagnetism is necessary for commercial applications.

Although large effort has been done during recent years all over the world to prepare room tem-

perature ferromagnetic III-V semiconductors [4], no satisfying material has been fabricated as so far. Either ferromagnetism is observed only at below room temperature (e.g. in GaMnAs and InMnAs [4]) or no ferromagnetic ordering is detectable (e.g. in GaMnN) [5]. On the other hand, it has been demonstrated that, during the growth of magnetic III-V semiconductors, ferromagnetic (often at room temperature) precipitates are fairly easily produced, yielding multi-phase materials [6]. Epitaxially grown $\text{Mn}_x\text{Si}_{1-x}$ ($x = 5$ at. %) thin film produces a material with anomalous Hall effect around 70 K which suggests the presence of internal magnetization of local Mn spins [7].

Ion implantation has also been utilized to achieve ferromagnetism in semiconductor crystals. Ferromagnetic ordering in silicon implanted with Mn^+ ions (Si:Mn) has been reported recently; this ordering is evidently related to the structure of Mn-enriched near-surface layer in implanted material [8]. It has been found that, for Si:Mn produced by implantation with Mn^+ doses, $D = 10^{15} - 10^{16} \text{ cm}^{-2}$, at energy, $E = 300 \text{ keV}$, Curie temperature exceeds 400 K after rapid thermal annealing at 1070 K. Ferromagnetic properties of annealed Si:Mn have been attributed to creation of $\text{MnSi}_{1.7}$ [9]. As it has been stated earlier [10, 11], not only temperature, but also *HP* applied at processing of implanted silicon affect structural and ferromagnetic properties of DMS.

This paper is focused on investigation of the defect structure of GaMnAs and Si:Mn subjected to annealing.

Experimental

001 oriented GaMnAs was grown by the MBE or ALE (Atomic Layer Epitaxy) methods. Layer thickness and Mn concentration for investigated samples as well as temperature of substrate during growth are presented in Table 1. Si:Mn was prepared by implantation of the Czochralski silicon with Mn^+ ($D = 1 \times 10^{16} \text{ cm}^{-2}$, $E = 160 \text{ keV}$). The projected ion range of Mn^+ (R_p) in the implanted samples was equal to 140 nm; $\Delta R_p = 50 \text{ nm}$. Substrate temperature during implantation was equal to 610 K.

The samples were subjected to processing at various temperatures (T , up to 670 K for GaMnAs and up to 1270 K for Si:Mn, processing for 1 h) under ambient (10^5 Pa) and high hydrostatic pressure ($HP = 1.1 \text{ GPa}$) in argon atmosphere.

The defect structure of samples was determined by high resolution X-ray diffraction methods

using the conventional and synchrotron radiation sources (HASYLAB-DESY). Conventional X-ray investigations were carried out using MRD-PHILIPS diffractometer in the double (DAD) and triple (TAD) axis configurations. Lattice parameters for GaMnAs, before and after the treatment, were measured. Reciprocal space maps (RSMs) for (004) symmetrical reflections of Si:Mn were registered. Simulations of RSMs were performed using kinematical theory of X-ray diffraction.

Table 1
Investigated $\text{Ga}_{1-x}\text{Mn}_x\text{As}$ layers and relative decrease of out-of-plane lattice parameters ($\Delta a/a$) after *HP-T* treatment. Samples A66, A94 were grown by MBE method; sample A144 — by ALE method.

Sample	Layer thickness [μm]	Mn concentration [%]	Substrate temp. [K]	$\Delta a/a$
A66	0.8	2	500	0.0017
A94	0.8	5.5	490	0.0068
A144	0.3	10	430	0.0086

Atomic Force Microscopy measurements (AFM) were performed with Digital Instrument in tapping mode; the root mean square (RMS) roughness was determined (RMS is defined as a standard deviation of the roughness in the direction perpendicular to the surface). Secondary Ion Mass Spectroscopy (SIMS) was used for determination the Mn depth profile.

Results and discussion

a) GaMnAs samples

The X-ray $2\theta/\omega$ scans (004 reflection) for the as-grown and *HP-T* treated GaMnAs layers are presented in Fig. 1. The layer thickness, calculated before and after the treatment from the interference fringe distance, was practically the same. However, the positions of 004 peaks coming from the layers were shifted into direction of the GaAs peak. It means that the out-of-plane lattice parameters of layers (a_{GaMnAs}) decrease. The out-of-plane lattice parameter of the A144 sample was equal to the lattice parameter of the substrate, but for the A66 sample was smaller than that of GaAs (Fig. 1). Layer of the sample A66 is under tensile strain. It is worth to mention that Mn concentration remained unchanged before and after the treatment (SIMS results).

AFM images for the A94 sample show on a creation of precipitates at the surface (Fig. 2). The structure and composition of these precipitates remains still unknown.

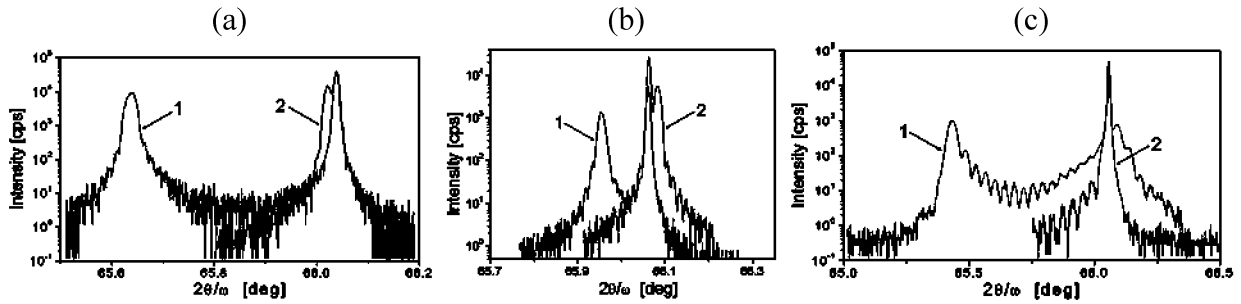


Fig. 1. $2\theta/\omega$ scans (004 reflection) of as-grown (1) and *HP-T* (2) treated GaMnAs for samples: A94 (a), A66 (b) and A144 (c).

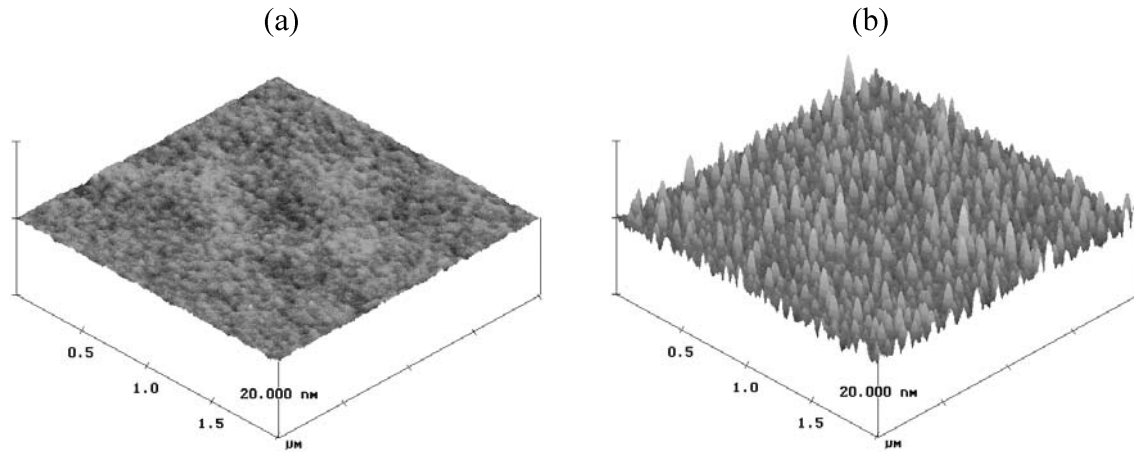


Fig. 2. AFM images of A94 sample surface before (a) and after (b) treatment.

Contraction of the lattice parameter can be related to the decreased concentrations of interstitial Mn atoms and / or of arsenic antisites. The contribution of arsenic antisites and of Mn atoms, both substitutional and interstitial, to the a_{GaMnAs} value is given by the formula [12]:

$$a_{\text{GaMnAs}}(x,y,z) = a_0 + 0.02x + 0.69y + 1.05z$$

where: a_0 — lattice constant of defect-free GaAs, y — concentration of As antisites, z — concentration of Mn in the interstitial positions.

Taking into account the high concentrations of Mn interstitials and of antisites, related to the high Mn concentration and growth of GaMnAs at low temperature, the decreased concentrations of interstitial Mn atoms and of arsenic antisites can be assumed to be responsible for the decreased lattice parameters. However, removal of interstitials can not explain experimental result: the layer lattice parameter is lower than that of the substrate in the case of sample A66. A creation of MnAs nanoclusters can modify diffraction from the layer which

indicates change of strain (from compressive to tensile) in the layers [13, 14]. A creation of hexagonal MnAs nanoclusters has been observed for the GaMnAs sample subjected to rapid thermal annealing at about 970 K; zincblende Mn(Ga)As clusters have been reported to grow at 870 K in effect of annealing under MBE conditions [14]. In both cases the matrix develops a small tensile strain of similar value. Due to lower annealing temperature, a creation of zincblende nanoclusters only can be expected in our experiments.

b) Si:Mn samples

Synchrotron radiation in the grazing incident diffraction geometry was applied to examine the near-surface region of Si:Mn. The structure of Si:Mn was found to be dependent on T (Fig. 3). Partial re-crystallization of the near-surface (buried) area for the as-implanted sample is detected. The diffraction peaks 111, 220 and 422 coming from polycrystalline Si have been found (Fig. 3) (diffraction peak 311 at $2\theta = 55.5^\circ$ is asymmetric peak from

monocrystalline Si matrix). After the treatment at 610 K, the originally observed diffraction peaks, originating from polycrystalline Si, disappeared. However, for higher treatment temperature, 870 K, and $HP = 1.1$ GPa, the diffraction peaks originating from the presence of polycrystalline Si were observed (Fig. 3), evidencing gradual recovery of damages. In this case and also for the sample treated under ambient pressure, the peaks from the tetragonal Mn_4Si_7 phase were detected with the lattice parameters: $a = 5.525$ E and $c = 17.463$ E.

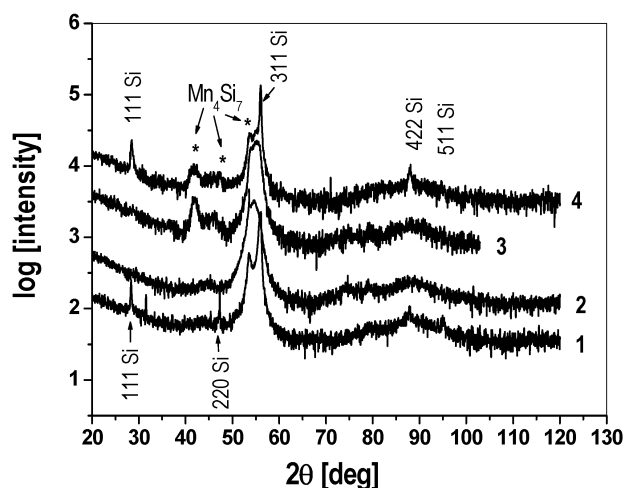


Fig. 3. Synchrotron radiation ($\lambda = 1.54056$ E) 2θ scans in grazing incidence diffraction geometry for Si:Mn samples: 1 — as — implanted; 2 — treated under atmospheric pressure at 610 K; 3 — treated under atmospheric pressure at 870 K; 4 — treated at 870 K under 1 GPa. Reflexes originating from Mn_4Si_7 phase are marked by arrows.

The 004 reciprocal space maps of Si:Mn are presented in Fig. 4. The inserts in the figures present simulation of these maps. X-ray diffuse scattering was not observed for the samples treated at 610 K under 10^5 Pa (Fig. 4a). This scattering was very weak after the treatment under HP , showing on presence in the sample crystallites with preferred orientation. The presence of crystalline near-surface layer is responsible for enhanced diffuse scattering from the samples annealed at high temperature (Fig. 4b). From simulation of RSM's it follows that processing at 1270 K results in a creation of weak type of defects for example dislocation loops or of stacking faults [15]. The surface of samples after annealing remains unchanged as follows from the AFM images. The depth profiles of Mn were practically unchanged after the $HP-T$ treatment.

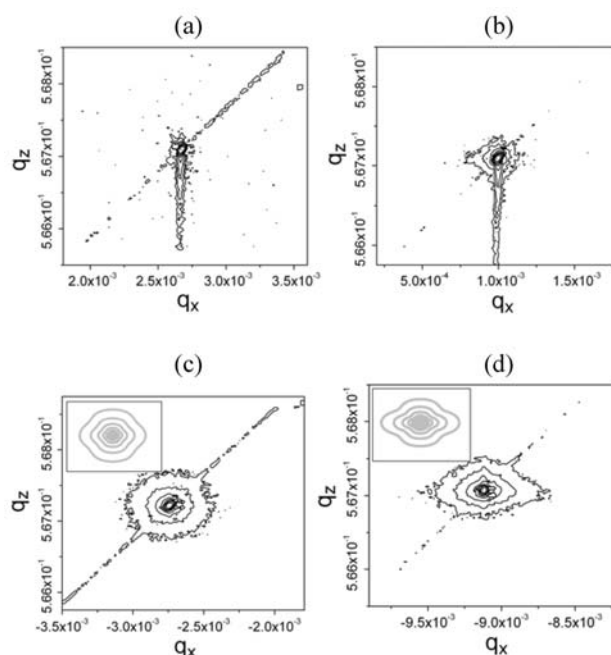


Fig. 4. 004 reciprocal space maps of Si:Mn treated for 1 h: (a) at 610 K under atmospheric pressure; (b) at 610 K under 1.1 GPa; (c) at 1270 K under atmospheric pressure; (d) at 1270 K under 1.1 GPa.

Conclusions

In the case of GaMnAs layer treated at about of 600 K under enhanced pressure, the lattice parameters decreased. This decrease of lattice parameters is probably related to the smaller concentration of As antisites and of Mn interstitials in the GaMnAs lattice. The strain changes from compressive to tensile are related to a creation of precipitates.

The temperature-pressure treatment makes it possible to modify the Si:Mn structure. The tetragonal Mn_4Si_7 phase has been formed in processed Si:Mn; the lattice a and c parameters of Mn_4Si_7 were determined. More pronounced re-crystallization of amorphous material was observed for the sample annealed under enhanced pressure. Enhanced pressure applied at processing affects also diffusivity of Mn atoms as well as of Si interstitials and vacancies. On the basis of X-ray diffraction and RSM simulation the defect structure of Si:Mn was determined.

Acknowledgements

The work was partially supported by the Ministry of Education and Science of Poland under the grant No. N20205232/1189.

List of references

1. Ohno O., Ferromagnetic semiconductors for spintronics // *Physica B* — 2006. — No. 376-377. — P. 19-21.
2. Ohno O., Making Nonmagnetic Semiconductors Ferromagnetic // *Science* — 2006. — No. 281. — P. 951-956.
3. Matsukura F., Ohno H., Shen A., Sugarawa Y., Transport properties and origin of ferromagnetism in (Ga,Mn)As // *Phys.Rev. B* — 1998, No 57. — P. R2037-R2040.
4. Dietl T., Ohno H., Matsukura F., Cibert J., Ferrand D., Zener Model Description of Ferromagnetism in Zinc-Blende Magnetic Semiconductors, *Science* — 2000 — No. 287. — P. 1019-1022.
5. Zając M., Gosk J., Kamińska M., Twardowski A., Szyszko J., Podsiadło S., Paramagnetism and anti-ferromagnetic d-d coupling in GaMnN magnetic semiconductor, *Applied Phys. Letters*, — 2001-No.79. — P. 2432-2434.
6. Moreno M., Trampert A., Jenichen B., Daweritz L., Ploog K., Correlation of structure and magnetism in GaAs with embedded Mn(Ga)As magnetic nanoclusters. *J. Appl. Phys* — 2002 — No. 92. — P. 4672-4676.
7. Nakayama H., Ohta H., Kulatov E., Growth and properties of super-doped Si:Mn for spin-photonics // *Phys. B* — 2001 — No.302-303. — P. 419-424.
8. Bolduc M., Awo-Affouda C., Stollenwerk A., Huang M.B., Ramos F.G., Agnello G., LaBella V.P., Above room temperature ferromagnetism in Mn-ion implanted Si // *Phys. Rev. B* — 2005. — No. 71. — P. 033302-1 — 033302-4.
9. Shegqiang Zhou, Potzger K., Gufei Zhang, Mucklich A., Eichhorn F., Schell N., Grotzschel R., Schmidt B., Skorupa W., Helm M., Fassbender J., Geiger D., Structural and magnetic properties of Mn-implanted Si // *Phys. Rev.B* — 2007 — No 75. — P. 0852003-1 — 085200-6,
10. Misiuk A., Bak-Misiuk J., Surma B., Osinniy W., Szot M., Story T., Jagielski J., Structure and magnetic properties of Si:Mn annealed under enhanced hydrostatic pressure // *J. Alloys Comp.* — 2006. — No.423. — P. 201-204.
11. Misiuk A., Surma B., Bak-Misiuk J., Barcz A., Jung W., Osinniy W., Shalimov A., Effect of pressure annealing on structure of Si:Mn // *Mater. Sci. Semicond. Process.* — 2006. — No.9. — P. 270-274.
12. J. Masek, J. Kurdnowsky, F. Maca, Lattice constant in diluted magnetic semiconductors (Ga,Mn)As // *Phys. Rev.B.* — 2003 — No.67 — P.153203-153206.
13. Moreno M., Kaganer V.M., Jenichen B., Trampert, L. A. Daweritz L., Ploog K., Micromechanics of MnAs nanocrystals embedded inGaAs // *Phys.Rev.B* — 2005 — No.72. — P.115206-1 — 115206-8.
14. Moreno M., Jenichen B., Daweritz L., Ploog K., Lattice distortion of MnAs nanocrystals embedded in GaAs : Effect on magnetic properties // *Appl. Phys. Lett.* — 2005 — No. 86 — P. — 161903-1 — 161903-3.
15. Holy V., Pietsch U., Baumbach T., High resolution X-Ray scattering from thin films and multilayers — Germany, Berlin.: ed. by Springer Tracts in Modern Physics, 1998 — 170 p.